Evolutionary properties of stellar standard candles: Red clump, AGB clump and white dwarfs

Maurizio Salaris

Astrophysics Research Institute, Liverpool John Moores University, 12 Quays House,
Birkenhead, CH41 1LD, UK
email: ms@astro.livjm.ac.uk

Abstract. The location of the white dwarf cooling sequence in the colour–magnitude diagram of simple stellar populations, the magnitude of the red clump and the magnitude of the asymptotic giant branch clump are three stellar distance indicators based on advanced evolutionary phases of low-mass stars. With the present observational capabilities, they can be applied to reach distances ranging from the Galactic disk and halo populations, to galaxies within the Local Group. Techniques devised to exploit these distance indicators are presented, together with a discussion of their calibration and the main sources of systematic errors. A first semi-empirical calibration of the asymptotic giant branch absolute magnitude in both the I and K bands is also derived.

Keywords. stars: AGB and post-AGB, stars: distances, stars: horizontal- branch, white dwarfs

1. Introduction

Deep colour–magnitude diagrams (CMDs) of stellar populations, combined with results of stellar evolution theory, provide three distance indicators that make use of He-core burning and post-He-core burning low-mass stars. With current observational capabilities, they can be applied to reach distances ranging from the Galactic disk and halo populations, to galaxies within the Local Group. These three 'cosmic rulers' are the CMD location of bright white dwarfs (WDs), the magnitude of the red clump (RC) and the magnitude of the asymptotic giant branch (AGB) clump. A basic description of the techniques employed to exploit WDs, RC and AGB clumps as distance indicators is presented in the next sections.

2. White Dwarfs

WD cooling sequences were first applied as distance indicators to determine distances to Galactic globular clusters (GGCs) by Renzini *et al.* (1996). The standard candle is, in this case, a template local WD sequence with effective temperature ($T_{\rm eff}$) ranging between 10,000 and 20,000 K, and precise parallax measurements, which is matched to a dereddened cluster WD sequence. This 'WD-fitting' technique, is analogous to the classic main-sequence (MS)-fitting technique. A key assumption of this method is that the local template WD sequence is equivalent to the cluster counterpart. If this is the case, the main advantage of the WD-fitting technique over MS fitting is that it is in principle (barring metallicity-dependent initial–final-mass relationships) independent of the initial chemical composition of the globular cluster, since all WDs have virtually metal-free atmospheres. Given that in the local field the ratio between DA (H-dominated atmospheres) and non-DA (He-dominated atmospheres) WDs is roughly 4:1, the template

145

WD sequence is typically made of spectroscopically identified DA objects, assuming that in star clusters DA objects are also predominant in the relevant effective temperature range.

All stars in a GGC are approximately coeval; therefore, the luminosity (and, thus, $T_{\rm eff}$) of a WD of a given mass is constrained by the fact that the sum of its cooling age ($t_{\rm cool}$) plus the evolutionary time of the progenitor ($t_{\rm prog}$) must be equal to the cluster age ($t_{\rm cl}$). One also has to assume an initial–final-mass relationship. The left-hand panel of Fig. 1 displays the WD cooling sequence (H-atmosphere WDs) of an old cluster with initial solar metallicity and ages of 10 and 12 Gyr, respectively, in the M_V–$(B - V)$ plane, as predicted by the theoretical isochrones of Salaris *et al.* (2000). The adopted initial–final-mass relationship provides WD masses which are nearly constant and equal to 0.54 $M_\odot$ for progenitor masses up to ∼2.5 $M_\odot$, and then increase up to 1.0 $M_\odot$ when the progenitor mass reaches 7.0 $M_\odot$. This is consistent, e.g., with the semi-empirical determination by Salaris *et al.* (2009).

The sequences show a pronounced turn to the blue at their dimmer end which, as the age of the cluster increases, is located at increasingly fainter magnitudes. Until this blue turn, the WD sequence is almost coincident with the cooling track of the ∼0.54 $M_\odot$ WDs, whilst the blue turn is caused by the contribution of more massive WDs. It is easy to understand this behaviour by recalling that at each brightness along the cooling sequence $t_{\rm cl} = t_{\rm cool} + t_{\rm prog}$. Given that $t_{\rm cool}$ is very short at the bright end of the cooling sequence, and negligible with respect to $t_{\rm GC}$, $t_{\rm prog}$ – hence, the progenitor mass – has to be (to a very good approximation) constant for a large magnitude range, and very close to the MS turn-off mass.

There are, in principle, four parameters that can introduce a systematic error in the WD-fitting distance estimates, when there are significant differences between the properties of the local template WD sequence and the cluster counterpart:
   (i) The mass of the WD cooling sequence;
   (ii) The thickness (in mass) of the envelope;
   (iii) The chemical composition of the envelope (DA, non-DA);
   (iv) The chemical stratification of the core (different CO profiles).
The effects of these parameters have been addressed by Salaris *et al.* (2001) in the M_V–$(B - V)$, 'BV', and M_V–$(V - I)$, 'VI', diagrams, which are actually the most popular CMDs employed for studying cluster WDs.

If the template and cluster sequences (in the relevant $T_{\rm eff}$ range) are populated by WDs of different masses (owing to, e.g., a different initial–final-mass relationship), the more massive sequence is shifted to larger M_V values, because of their smaller radii. The derivative $\Delta M_V / \Delta(M/M_\odot) = 2.3$ for masses between 0.45 and 0.60 $M_\odot$.

Evolutionary calculations suggest that DA WDs form with hydrogen layers of mass fraction $q(\rm H)$ equal to $\log q(\rm H) = -4.0$, even though much smaller values (by orders of magnitude) can also be inferred from asteroseismology of field objects. The value of $q(\rm H)$ in cluster WDs cannot yet be constrained empirically. A reduction of the thickness of the H envelope shifts the track – at constant colour – towards larger M_V values, with a derivative $\Delta M_V / \Delta \log q(\rm H) \sim -0.035$ for $\log q(\rm H)$ ranging between -4.0 and -7.0.

The right-hand panel of Fig. 1 displays BV and VI CMDs for 0.54 $M_\odot$ DA (represented by a pure H atmosphere) and non-DA (represented by a pure He atmosphere) models, in the $T_{\rm eff}$ range between 10,000 and 20,000 K.

The thickness of the H envelope is $\log q(\rm H) = -4$, whilst the He envelope has a mass ratio $\log q(\rm He) = -3.5$. Note the very different behaviour of the tracks in the BV and VI planes, due to the effect of the different compositions on the bolometric corrections.
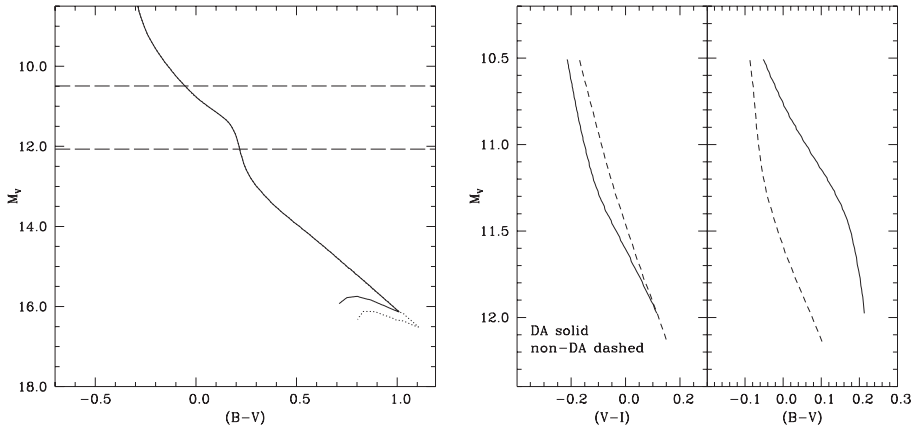
Figure 1. (left) CMD of two cluster WD cooling sequences with ages $t = 10$ (solid line) and 12 Gyr (dotted line), and solar metallicity. The horizontal dashed lines mark the region for T_{eff} between 10,000 and 20,000 K. (right) BV and VI CMDs for 0.54 $M_\odot$ DA and non-DA (represented by a pure He atmosphere) models, in the T_{eff} range between 10,000 and 20,000 K.

Finally, a variation of the internal CO stratification, due to uncertainties in the treatment of core mixing during the core-He-burning phase and/or in the $^{12}C(\alpha, \gamma)^{16}O$ reaction rate – within realistic limits – has a very minor impact on the cooling sequence in this effective temperature range compared to the effects previously discussed. Based on these properties, Monte Carlo simulations by Salaris *et al.* (2001) that considered 'realistic' uncertainties in the distribution of these parameters in synthetic template and cluster WD sequences conclude the following.

(*a*) The unknown thickness of the H layers in cluster DA WDs plays a non-negligible role, comparable to the role played by uncertainties in the WD masses. For reasonable assumptions (derived from observations of field WDs and constraints from cluster CMDs) about the unknown mass and $\log q(H)$ values in cluster DA WDs, estimates of the maximum systematic error in the derived distance moduli are within ~ 0.10 mag. However, one should be aware that particular combinations of WD masses and envelope thicknesses – still allowed by the current weak or non-existent observational constraints – could produce larger errors.

(*b*) A photometric precision better than ~ 0.05 mag is needed to distinguish DA from non-DA WDs in the BV plane. An even higher precision is needed when using the VI plane. For larger observational errors and no clear (spectroscopic) distinction between DA and non-DA cluster WDs, fitting a template DA sequence to a cluster sequence made of a mixture of DA and non-DA stars introduces a very small systematic error ~ -0.03 mag in the VI plane, but this error increases to $\sim +0.20$ mag, in the BV plane. The VI plane looks, therefore, much better suited for the application of the WD-fitting method, since it allows to get rid of the uncertainty caused by possible contamination of the DA sample by non-DA white dwarfs.

(*c*) Contamination by He-core WDs should not influence appreciably the derived distances.

3. Red clump

RC-based distances – which with current observational capabilities can reach extragalactic objects within the Local Group – have been the subject of several investigations,

spurred by the publication of the *Hipparcos* parallax catalogue. The RC appears in the CMDs of populations with ages older than ∼0.5–1 Gyr as a clump of red stars close to the red giant branch (RGB; see Fig. 2). It is populated by objects in the central He-burning phase, that have ignited He in an electron-degenerate core (or around the transition to non-degeneracy), i.e. they are the equivalent of horizontal branch (HB) stars in GGCs. In fact, the HB of metal-rich GGCs is usually – but not always – a RC (47 Tuc is a 'classic' example).

Some very general properties of the RC in the VIK bands (for which solid calibrations of the local RC absolute magnitudes exist) can be summarized as follows:

(*a*) At fixed age, theoretical RC star models become redder with increasing metallicity. The bolometric magnitude, and the magnitudes in the V and I bands become fainter with increasing metallicity when age is fixed. The reverse is true for the K band. This different behaviour is due to the effect of the bolometric corrections.

(*b*) At fixed metallicity, RC models cover a limited range of luminosities in all filters, on the order of 0.2–0.3 mag. When the age decreases from 3 to 1 Gyr, the luminosity decreases, owing to the transition between degenerate and non-degenerate He cores at He ignition, followed by a sharp increase at an age of 0.5 Gyr, which signals the complete removal of electron degeneracy in the He cores.

After the *Hipparcos* results, the mean absolute magnitude of the local RC can now be measured in VIK with a precision on the order of 0.01 mag, and used as zero point of the RC distance scale. The determination of the absolute magnitude of the local RC in a given passband λ ($M_{\lambda,\mathrm{local}}^{\mathrm{RC}}$) and the apparent magnitude $m_{\lambda}^{\mathrm{RC}}$ of the RC in a given stellar population are straightforward, since in both the *Hipparcos* database of local stars and in CMDs covering even small fractions of nearby galaxies, one can find several hundreds of RC objects. Following Stanek & Garnavich (1998), a non-linear least-squares fit of the
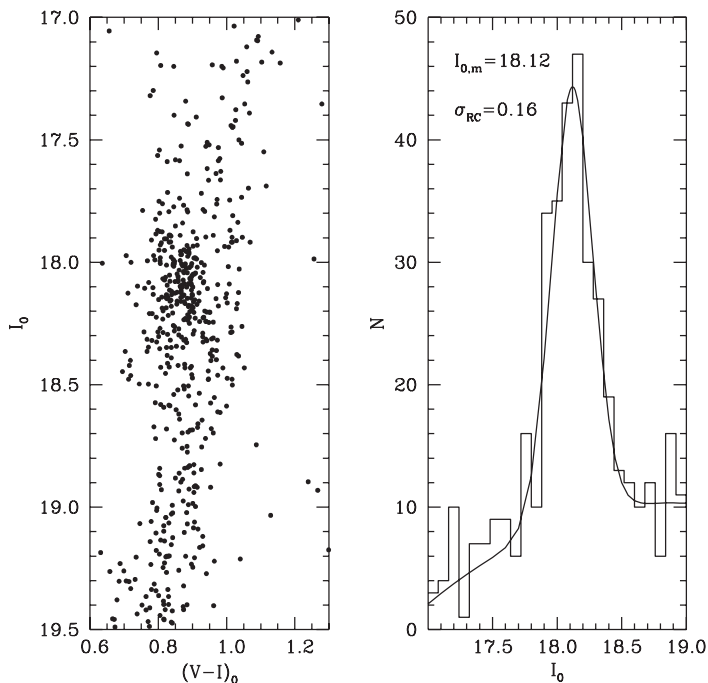

Figure 2. Observed CMD of the RC region of an LMC field and the fit to the corresponding luminosity function to determine the RC level.

function

$$N(m_\lambda) = a + bm_\lambda + cm_\lambda^2 + d \exp\left[-\frac{(m_\lambda^{\mathrm{RC}} - m_\lambda)^2}{2\sigma_{m_\lambda}^2} \right]$$

to the histogram of stars in the RC region per magnitude bin provides the value of m_λ^{RC} and its associated standard error (see Fig. 2). The analysis by Alves *et al.* (2002) has provided, for the local RC, $M_{V,\mathrm{local}}^{\mathrm{RC}} = 0.73 \pm 0.03$ mag, $M_{I,\mathrm{local}}^{\mathrm{RC}} = -0.26 \pm 0.03$ mag and $M_{K,\mathrm{local}}^{\mathrm{RC}} = -1.60 \pm 0.03$ mag.

Once m_λ^{RC} has been measured in a nearby galaxy, distance moduli, $\mu_0 = (m - M)_0$, are derived from

$$\mu_0 = m_\lambda^{\mathrm{RC}} - M_{\lambda,\mathrm{local}}^{\mathrm{RC}} - A_{m_\lambda} + \Delta M_\lambda^{\mathrm{RC}}.$$

Here, A_{m_λ} denotes the interstellar extinction to the target RC population, and

$$\Delta M_\lambda^{\mathrm{RC}} = M_{\lambda,\mathrm{local}}^{\mathrm{RC}} - M_{\lambda,\mathrm{target}}^{\mathrm{RC}}$$

is the 'population correction', i.e. the difference of the mean RC absolute magnitude between the local and target samples of stars. Given the complex behaviour of M_λ^{RC} as a function of age and metallicity, accurate RC-based distances need a proper evaluation of $\Delta M_\lambda^{\mathrm{RC}}$. This population correction is expected to be strongly dependent on the star-formation history (SFH) of the target and local populations. The papers by Girardi *et al.* (1998), Girardi & Salaris (2001) and Salaris & Girardi (2002) have tackled this issue from a theoretical point of view, by making use of synthetic CMDs to investigate in detail the expected dependence of the RC mean magnitude in several photometric filters as a function of age and metallicity in single-age, single-metallicity populations. They also modelled composite stellar systems like the solar neighbourhood, the LMC and SMC, employing literature SFHs, and calculated the corresponding 'population corrections' $\Delta M_\lambda^{\mathrm{RC}}$.

Synthetic models of the local RC reproduce well the observed distribution of stellar magnitudes, colours and [Fe/H], and their correlations or absence thereof. These theoretical population corrections employ theory only in a differential sense. Both $M_{\lambda,\mathrm{local}}^{\mathrm{RC}}$ and $M_{\lambda,\mathrm{target}}^{\mathrm{RC}}$ are calculated from synthetic CMDs employing the appropriate SFH, but it is only their difference that determines $\Delta M_\lambda^{\mathrm{RC}}$. Fig. 3 displays the predicted $\Delta M_\lambda^{\mathrm{RC}}$ values in the VIK bands for a large range of single-age, single-metallicity populations. These have been tested empirically by Percival & Salaris (2003) using a sample of eight Galactic open clusters harbouring RC stars, plus the GGC 47 Tuc. These authors have determined cluster distances – hence the RC absolute magnitudes in V, I and K – by means of a MS-fitting method that uses a large sample of local field dwarfs with accurate *Hipparcos* parallaxes, and determined their MS turn-off ages. They have, finally, calculated the corresponding empirical values of $\Delta M_\lambda^{\mathrm{RC}}$ considering the empirical absolute magnitudes of the local RC. A comparison with the theoretical population corrections displayed in Fig. 3 for the appropriate ages and metallicities reveals agreement at the level of $\sim$0.1 mag. Empirical calibrations of M_λ^{RC} versus [Fe/H] relations determined in systems harbouring composite stellar populations need to be treated with caution. Depending on the procedure followed, they may be completely dependent on the specific SFH of the stellar system used as calibrating sample, and do not have any general validity. The best empirical approach has been followed by Pietrzyński *et al.* (2010), who have compared RC magnitudes with the I-band magnitude of the tip of the RGB (generally weakly sensitive to the galaxy's SFH) in a sample of 23 galaxies in the Local Volume. They found strong population effects in the V and I magnitudes of RC stars, confirming the theoretical results of Girardi & Salaris (2001). The following summary of the

properties of the RC population corrections may serve as guidelines to the use of the RC as distance indicator:

(a) In a composite stellar population, the age (mass) distribution of stars in the RC depends in a complex way on the population's SFH, the trend of He-burning timescale with stellar mass and metallicity, and the initial mass function. As an example, for a uniform SFH between 0.1 and 10 Gyr in the past (at constant metallicity), the RC population is dominated by ~1.5 Gyr-old objects, which will provide the largest contribution to $M_{\lambda,\mathrm{target}}^{\mathrm{RC}}$.

(b) The value of $\Delta M_{\lambda}^{\mathrm{RC}}$ is strongly dependent on both the SFH of the target population and the photometric filter. For example, for the RC in the LMC, the predicted population corrections amount to ~0.2 mag in I, but only ~ −0.03 mag in K.

(c) K-band obervations are best to determine RC distances to populations with a generic SFH that does not decrease with decreasing lookback time. In this case, irrespective of the detailed shape of the SFH, the RC will always be dominated by objects with ages around 2 Gyr, and the population correction is practically negligible. I-band data are best for old (but subsolar-metallicity) populations. Under these conditions the value of $\Delta M_{\lambda}^{\mathrm{RC}}$ is close to zero.

4. AGB clump

At the end of core He burning in low-mass stars, models predict a fast luminosity increase after central He exhaustion, followed by a temporary drop and a subsequent monotonic rise until the beginning of the thermal-pulse phase. As a consequence, one expects that the transition from core to shell He burning is marked by a gap in star counts, followed by a well-defined clump of objects that mark the beginning of the AGB,
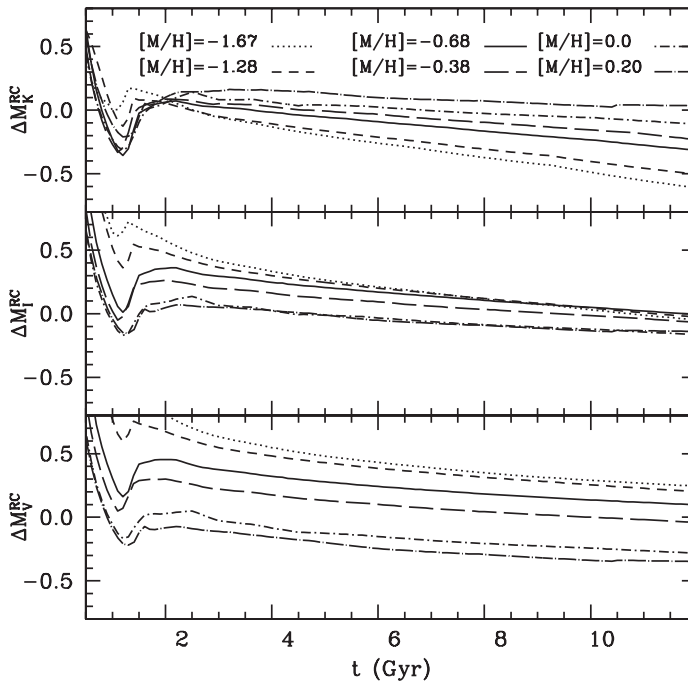

Figure 3. Population corrections to the local RC magnitudes in the V, I and K bands, for the labelled ages and metallicities (scaled-solar mixture).

the so-called AGB clump, a local maximum in the star counts as a function of magnitude, like for the RGB bump. Stars cross the same luminosity interval three times, hence resulting in the AGB clump feature.

This prediction is nicely confirmed by observations of well-populated GGCs such as 47 Tuc (see, e.g., the CMD of Beccari *et al.* 2006). The bolometric luminosity of the AGB clump is expected to depend significantly on the evolving stellar mass: higher masses tend to generate brighter (and redder) AGB clumps. This also implies an indirect dependence on all parameters that can affect the mean mass and its distribution along the previous HB phase, i.e. the RGB mass-loss efficiency, but also the initial metallicity and cluster age. In particular, moving from metal-rich to metal-poor stellar populations, the AGB clump is expected to become cooler and less clumpy with decreasing stellar mass. This makes the identification of this feature in the CMDs of metal-poor stellar systems less obvious. The properties of the AGB clump have been discussed by, e.g., Castellani *et al.* (1991).

From an observational point of view, one needs to also take into account the effect of the bolometric corrections which, depending on the selected photometric band, may enhance or erase the dependence of the AGB-clump magnitude on the evolutionary parameters of the parent stellar population. Here we present a first semi-empirical calibration of the AGB-clump absolute magnitude in the I and K bands, useful for distance determinations to old stellar populations. It is based first on the determination of the absolute magnitude of the AGB clump in 47 Tuc. The apparent I (Cousins) magnitude is obtained from the CMD of Beccari *et al.* (2006), whilst the apparent K magnitude (transformed to the Bessell & Brett system) is from the CMD of Salaris *et al.* (2007). One obtains $M_{I,\text{AGB clump}}^{47\ \text{Tuc}} = -1.20 \pm 0.06$ mag and $M_{K,\text{AGB clump}}^{47\ \text{Tuc}} = -2.73 \pm 0.09$ mag, assuming a distance modulus $(m - M)_0 = 13.23 \pm 0.08$ mag obtained from analysis of the eclipsing
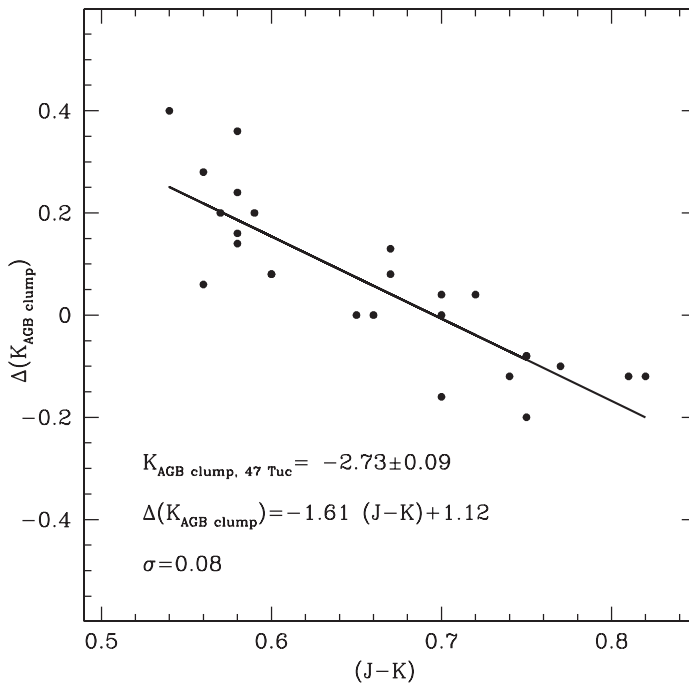

Figure 4. Population correction to the AGB clump of 47 Tuc in the K band, as a function of the $(J - K)$ colour (see text).

binary V69-47 Tuc by Thompson *et al.* (2010), and $E(B - V) = 0.04$ mag. Synthetic CMD simulations based on the BASTI stellar models (Pietrinferni *et al.* 2004, 2006) have been used to calculate the predicted magnitude differences ΔK and ΔI between the AGB clump in populations of varying ages and chemical compositions (i.e., this is the equivalent of the population corrections for the RC, where theory is employed only differentially) and the clump in 47 Tuc (assuming an age of 11 Gyr, [Fe/H] = -0.7 dex and [α/Fe]=0.40 dex for the clusters). One obtains the following relationships:

$$\Delta(K_{\mathrm{AGB\ clump}}) = -1.61\ (J - K) + 1.12,$$

valid for ages between 2 and 14 Gyr, [Fe/H] between solar and -2 dex, both for scaled-solar and α-enhanced ([α/Fe]=0.40 dex) chemistry, and varying HB morphologies – shown in Fig. 4 – and

$$\Delta(I_{\mathrm{AGB\ clump}}) = -0.025 \pm 0.07$$

for ages older than 7 Gyr and [Fe/H] < -1.0 dex (both for scaled-solar and α-enhanced abundances) and varying HB morphologies.

References

Alves, D. R., Rejkuba, M., Minniti, D., & Cook, K. H. 2002, *ApJ*, 573, L51
Beccari, G., Ferraro, F. R., Lanzoni, B., & Bellazzini, M. 2006, *ApJ*, 652, L121
Castellani, V., Chieffi, A., & Pulone, L. 1991, *ApJS*, 76, 911
Girardi, L. & Salaris, M. 2001, *MNRAS*, 323, 109
Girardi, L., Groenewegen, M. A. T., Weiss, A., & Salaris, M. 1998, *MNRAS*, 301, 149
Percival, S. M. & Salaris, M. 2003, *MNRAS*, 343, 539
Pietrinferni, A., Cassisi, S., Salaris, M., & Castelli, F. 2004, *ApJ*, 612, 168
Pietrinferni, A., Cassisi, S., Salaris, M., & Castelli, F. 2006, *ApJ*, 642, 797
Pietrzyński, G., Górski, M., Gieren, W., Laney, D., Udalski, A., & Ciechanowska, A. 2010, *AJ*, 140, 1038
Renzini, A., *et al.* 1996, *ApJ*, 465, L23
Salaris, M. & Girardi, L. 2002, *MNRAS*, 337, 332
Salaris, M., García-Berro, E., Hernanz, M., Isern, J., & Saumon, D. 2000, *ApJ*, 544, 1036
Salaris, M., Cassisi, S., García-Berro, E., Isern, J., & Torres, S. 2001, *A&A*, 371, 921
Salaris, M., Held, E. V., Ortolani, S., Gullieuszik, M., & Momany, Y. 2007, *A&A*, 476, 243
Salaris, M., Serenelli, A., Weiss, A., & Miller Bertolami, M. 2009, *ApJ*, 692, 1013
Stanek, K. Z. & Garnavich, P. M. 1998, *ApJ*, 503, L131
Thompson, I. B., *et al.* 2010, *AJ*, 139, 329